Numerical studies on randomly distributed gold nano-net structures

J. Fang,[1] L. J. Prokopeva,[1,2] M. A. Alam,[1] V. M. Shalaev,[1] and A. V. Kildishev[1*]

[1]Birck Nanotechnology Center, School of ECE, Purdue University, West Lafayette, IN 47907 USA
[2]Novosibirsk State University, Novosibirsk, Russia
kildishev@purdue.edu

Abstract: A randomly distributed gold nano-net is studied numerically via FDTD simulations. The dispersion of gold is implemented through a generalized dispersive material (GDM) model built on Padé approximants. The simulation of the dispersive random nano-net structure demands both fine nanoscale geometry and large span area in order to cover the complexity of interactions at the scattering surface. Along with additional equations for dispersive response this poses a severe challenge in terms of an efficient numerical implementation, especially in 3D. To reduce the simulation time we studied and determined the minimal size of the individual 2D-frames, which can be calculated independently and in parallel on a multiprocessing system. The impact of the individual frame size on accuracy is analyzed for a representative nano-net sample.

Keywords: Gold nano-net, Generalized Dispersive Material (GDM), FDTD, Parallel computing.

1. Introduction

Random metal composite films, or specifically surface composites, have attracted a great deal of research interests recently [1]. Due to their broadband resonance and their fractal morphology, they can localize electromagnetic energy into nano-scale regions and produce large near-field enhancements extending from the ultraviolet to the mid-infrared [2]. This feature, besides the merits of simple and low-cost fabrication requirements, give rise to numerous applications, such as surface-enhanced Raman scattering spectroscopy (SERS) [3-5], surface enhance infrared absorption for sensing [6-7], enhanced solar cell efficiencies [8-9], and others. In particular, random gold nano-nets that have low metal coverage (such that they are highly transparent) but are still close to the percolation threshold (such that they exhibit good electrical conductance) could be a promising candidate for anode designs in coherent light trapping for thin-film photovoltaic devices [10]. It is shown that such gold nano-nets could be operated either above or below the percolation limit depending on the application and cell configuration [11]. However, due to the strongly coupled metallic elements, theoretical methods such as Bruggeman's effective medium theory (EMT) [12] and the Maxwell-Garnett theory (and modifications thereof) [13] can only provide limited guidance for the design of these films [14]. Therefore the numerical study based on full-wave analysis is of importance. Numerical simulations of random nano-net structures demand both fine nano-scale geometries for the very thin nanowires as well as a large span area in order to cover the complexity of the interactions at the scattering surface. Moreover, in time-domain the frequency dispersion of material is introduced with additional differential or integral equations (auxiliary differential equation method, ADE or recursive convolution method, RC), which also sufficiently increase the computational complexity of numerical schemes. In this paper we show FDTD simulations with two featured methods used to reduce the computational costs. First, we give references to the implementation of GDM model, which is used to effectively implement the frequency dispersion of gold to FDTD method. Second, we investigate the mi-

nimal representative size of the nano-net, which can be simulated as an isolated part without loss of accuracy; those parts are calculated in parallel without any interconnects between subdomains. Finally, we show the averaged far-field electromagnetic response for the gold nano-net.

2. Generalized dispersive material (GDM) model for gold

The film under study is composed of gold nanowires randomly arranged on a dielectric substrate. In order to describe the frequency dispersion of the permittivity of gold precisely and efficiently for time-domain methods, we employ a dispersive model for gold defined as the sum of a Drude term and two critical point terms (D2CP) [15]. The detailed function of this model is given as follows [16].

$$\varepsilon(\lambda)=\varepsilon_{\infty}+\frac{\lambda_d^2}{\lambda^2+i\lambda\Gamma_d}+\sum_{m=1,2}f_m\lambda_m\left(\frac{e^{i\varphi_m}}{\lambda_m-(\lambda+i\Gamma_m)}+\frac{e^{-i\varphi_m}}{\omega_m+(\lambda+i\Gamma_m)}\right) \tag{1}$$

where $\varepsilon_{\infty}=2.75$ and the remaining parameters are listed in Table 1:

Table 1: Parameters of Dispersive D2CP Model of Gold:

Drude term	λ_d[nm]	Γ_d [nm]	Critical point terms	m	f_m	λ_m [nm]	Γ_m [nm]	φ_m [°]
	140	17000		1	0.75	445	2400	-22
				2	1.55	325	950	-38.6

Our approach allows reducing the computational cost, which comes from the dispersion implementation, in two ways. First, the permittivity function of gold has smaller number of dispersion terms than conventional Drude-Lorentz models, usually employed in many other papers. Second, each of the dispersion term is implemented numerically with the effective GDM algorithm [17, 18]. A piece-wise constant recursive convolution scheme (PCRC2, see for example [19]) was used to ensure 2nd-order accuracy of the entire scheme. Fig. 1 demonstrates the tested numerical local response of the dispersion of gold. The figure shows that both the magnitude (Fig. 1(a)) and phase (Fig. 1(b)) terms agree well with the analytic D2CP model.

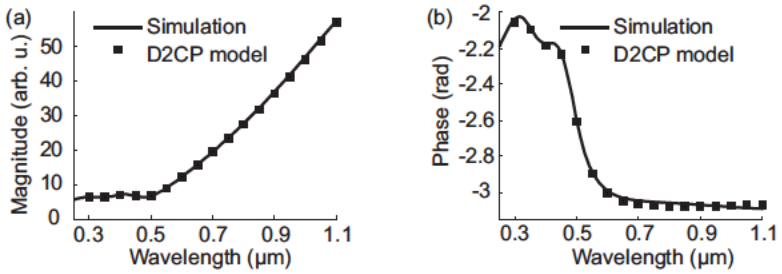

Fig. 1: The numerical local response of gold dispersion implemented through GDM algorithm (PCRC2 scheme) and compared with the analytical model (1).

3. Simulation for gold nano-net structure

The gold nano-net structure of interest is formed by 1-μm long gold nanowires with square cross-sections that are 40 nm wide on each side. The nano-net is supported by a silicon substrate ($\varepsilon_r = 3.5$) and are otherwise surrounded by air. The nanowires are randomly distributed in location and orientation, as shown in Fig. 2(a) and (b). We investigated the optical properties of such a gold nano-net under normal incidence from air, as shown in Fig. 2(c).

We are interested in the response of the nano-net system in a wavelength (λ) range from 0.3 to 4 μm, and hence the incident modulated Gaussian pulse was chosen as: $G(t)=\exp[-(t-t_0)^2/\tau^2]\sin\omega t$, where $\omega=2\pi c/\lambda$, $\tau=1$ fs, $t_0=3\tau$, and $\lambda=0.5$ μm. The spatial step size was $\Delta x=\Delta y=\Delta z=5$ nm with Courant condition number $\nu=0.5$, which gave us a time step $\Delta t=\nu\Delta x/c\sqrt{3}\approx 4.81\times10^{-18}$ s. The entire simu-

lation domain was 4 μm × 4 μm × 4 μm, truncated with perfectly matched layers (PMLs) in z direction and with periodic boundary conditions (PBCs) to all sides parallel to the *z* direction (see Fig. 2). The total-scattered field separation (TSFS) method was used to introduce the incident *x*-polarized plane wave into the simulation domain [20]. The time-domain reflected and transmitted field probes were recorded close to the source and to the shade sides of the domain along the propagation direction (*z* direction), and then averaged over the transverse cross-section. These probes were post-processed with an FFT to obtain the numerical far-field transmission (T) and reflection (R) spectra. Absorptance (A) was then obtained by calculating $A = 1 - T - R$.

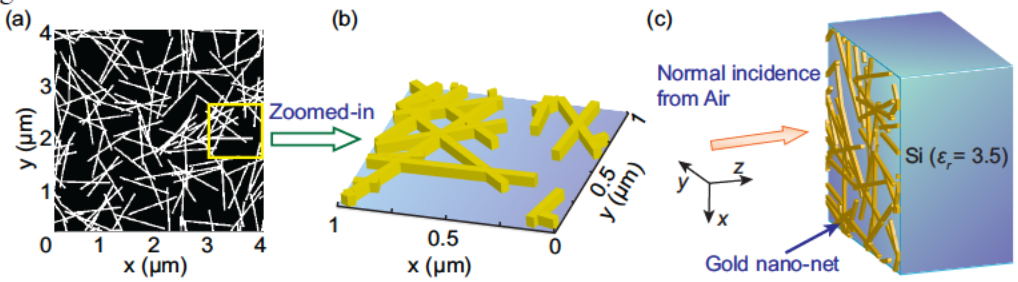

Fig. 2: Gold nano-net structure on Si: (a) top view of an entire simulated film, with white areas representing the gold nanowires, (b) zoomed-in 3D sketch of a portion of the gold nano-net, and (c) simulation model and coordinate definitions.

4. Optimal size of the individual frame

The direct sequential simulation of such a nano-net with given numerical parameters will demand for substantial computer resources, requiring huge RAM and considerable simulation time. One way to reduce the required computing resources is to use standard parallelization techniques for systems with shared and distributed memory. Scalability of work decomposition approach with OpenMP programming relies on availability of rather big shared memory machines and is subject to ineffective access to large data. Domain decomposition approach with MPI programming also allows for systems with distributed memory, but the scalability is then limited with interconnect capabilities, since the data from boundary cells shall be synchronized between processors via communication at each time step and the synchronization burden increases significantly with increase of number of processors involved, see [21]. Both limitations, ineffective access to large amount of data and interconnect burden, can be substantially decreased by using smaller individual frames, which are computed totally independently.

Here, we cut the initial sample into three different frame sizes: 2 μm × 2 μm, 1 μm × 1 μm, and 0.5 μm × 0.5 μm, as shown in Fig. 3, and set PBCs on each newly appeared boundary [22]. By comparing the simulation results one can find out the minimal size of the frame, for which the accuracy is still acceptable. The calculated spectra will vary widely from one individual frame to another due to differences in the local geometry; hence we obtained the macroscopic far-field spectral responses by the arithmetic averaging of the spectral data from each individual frame.

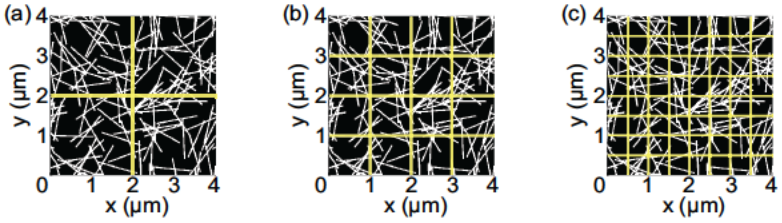

Fig. 3: Domain splitting with frame sizes of (a) 2 μm × 2 μm, (b) 1 μm × 1 μm, and (c) 0.5 μm × 0.5 μm.

In Figs. 4, 5, and 6, we show simulated far-field transmittance, reflectance and absorptance spectra for the three different aforementioned frame sizes. As we can see from Fig. 4, for 2 μm × 2 μm frame size the simulated far-field T, R and A spectra do not vary much from one individual frame to another, and

therefore this frame size is sufficiently large to contain the complexity of interactions at the scattering surface of the gold nano-net. In particular, the absorptance peak near 1 μm for all individual frames is consistent with the length the nanowire, and therefore we ascribe it to longitudinal plasmonic resonant modes along the length of the gold nanowires. The short-wavelength absorptance is related to inter-band transitions in the gold, which are accurately predicted in the D2CP model of gold.

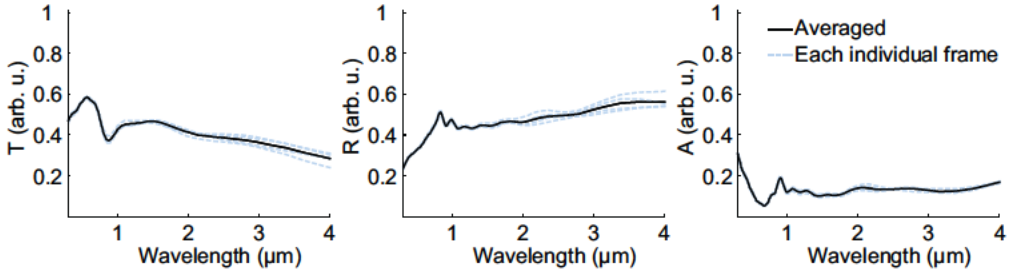

Fig. 4: Simulated far-field T, R and A with a frame size choice of 2 μm × 2 μm.

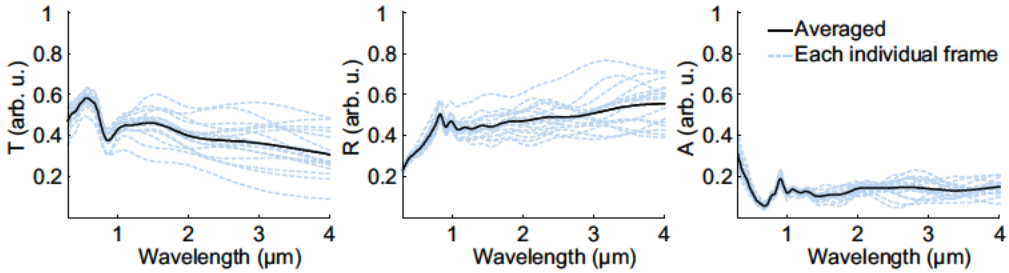

Fig. 5: Simulated far-field T, R and A with a frame size choice of 1 μm × 1 μm.

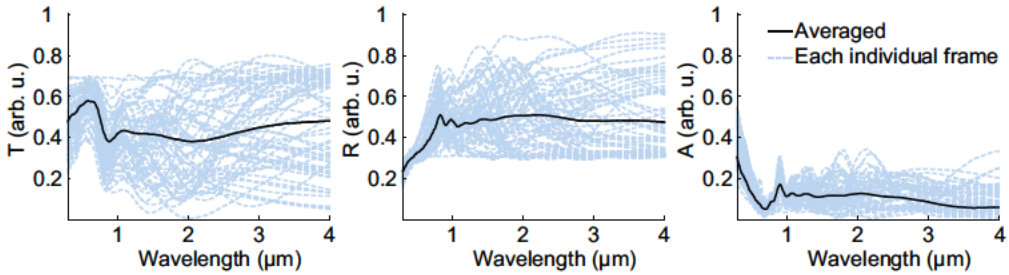

Fig. 6: Simulated far-field T, R and A with a frame size choice of 0.5 μm × 0.5 μm.

In Fig. 5 we used 1 μm × 1 μm independent frames. Although the simulated T/R/A spectra changes dramatically from one individual frame to another, the averaged T/R/A spectra converge to those for the larger 2 μm × 2 μm frames, as shown in Fig. 7. Furthermore, if we take even smaller 0.5 μm × 0.5 μm independent frame size, then the difference between T/R/A spectra of individual frames becomes larger, as illustrated in Fig. 6. An interesting phenomenon for 0.5 μm × 0.5 μm frame size case is that the averaged far-field T/R/A spectra converge to the larger frame size results only within the short-wavelength range (approximately for $\lambda < 1$ μm, as shown in Fig. 7). This is due to the fact that this frame size is too small to accurately represent nanowire coupling of longer waves meaning the absorptance resonances.

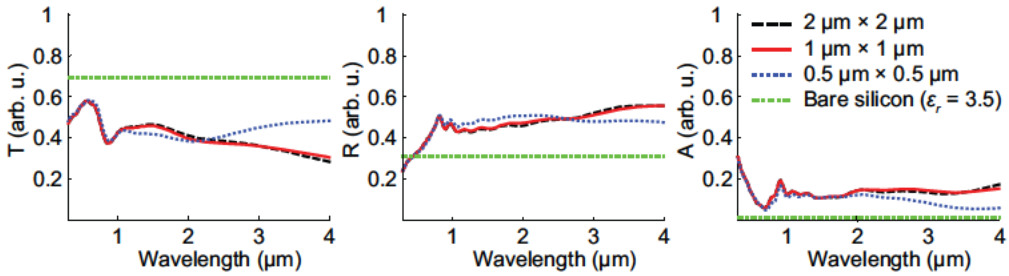

Fig. 7: Comparison of averaged far-field T, R and A with different frame size choices.

In addition, the far-field T/R/A spectra for bare silicon (assuming pure dielectric with $\varepsilon_r = 3.5$) is illustrated by green dash-dot line in Fig. 7, as we can see, the gold nano-net layer decrease the transmittance of the entire structure by 0.33, while increasing its reflectance and absorptance by 0.18 and 0.15 respectively across the whole spectrum.

This study shows that individual frame can be taken at least as small as 1 μm × 1 μm, which reduce the request on memory to 1/16 of the initial requirement. The reduction of the required size of RAM enlarges the choice of the hardware suited for the simulation, and may have a significant impact on effective memory access, resulting in less simulation time.

5. Conclusions

In summary, the optical properties of a randomly distributed gold nano-net sample have been studied numerically via FDTD simulations. For these simulations we have demonstrated two effective approaches to reduce the problem-specific large computational costs in terms of memory and long simulation times. First, we have implemented the dispersion of gold using the critical points model, with less dispersion terms compared to standard Drude-Lorentz models. Moreover, we have implemented this efficient dispersion model using a more economical GDM algorithm. Second, it is important to find the smallest possible size of representative 2D-frames, which could be calculated independently. This splitting approach, used on top of standard parallelization techniques for shared or distributed memory systems, is expected to provide the ultimate implementation for multiprocessor systems, as in the independent subdomains smaller amount of data can be accessed more effectively and the processor communications are not required. In the future, we will extend this problem-specific numerical study on minimal independent frame size and reveal theoretical prediction that long range correlations are distinct features for such gold nano-net composed by long metallic sticks [22]. Also we expect to use the proposed improvements of the numerical realization for simulation and optimization of complex random scattering surfaces for applications such as photovoltaic devices.

Acknowledgement

This work was partially supported by AFOSR FA9550-10-1-0264, ARO MURI Awards 50342-PH-MUR and NSF-DMR 1120923.

References

[1] A. K. Sarychev and V. M. Shalaev, "Electromagnetic field fluctuations and optical nonlinearities in metal-dielectric composites," *Phys. Rep.* Vol. 335, pp. 276-371, 2000.

[2] D. A. Genov, A. K. Sarychev and V.M. Shalaev, "Plasmon localization and local field distribution in metal-dielectric films," *Phys. Rev. E.* Vol. 67, pp. 056611-10, 2003.

[3] M. Moskovits, "Surface-enhanced spectroscopy," *Rev. Mod. Phys.* 57, pp. 783-826, 1985.

[4] K. Kneipp, Y. Wang, H. Kneipp, L.T. Perelman, I. Itzkan, R.R. Dasari and M.S. Feld, "Single molecule detection using surface-enhanced Raman scattering (SERS)," *Phys. Rev. Lett.* Vol. 78, pp. 1667-1670, 1997.

[5] V. P. Drachev, M. D. Thoreson, V. Nashine, E. N. Khaliullin, D. Ben-Amotz, V. J. Davisson and V. M. Shalaev, "Adaptive silver films for surface-enhanced Raman spectroscopy of biomolecules," *J. Raman Spec.* Vol. 36, pp. 648-656, 2005.

[6] A. Hartstein, J. R. Kirtley and J. C. Tsang, "Enhancement of the infrared absorption from molecular monolayers with thin metal overlayers," *Phys. Rev. Lett.* Vol. 45, pp. 201-204, 1980.

[7] D. Enders and A. Pucci, "Surface enhanced infrared absorption of octadecanethiol on wet-chemically prepared Au nanoparticle films," *Appl. Phys. Lett.* Vol. 88, pp. 184104-6, 2006.

[8] H. A. Atwater and A. Polman, "Plasmonics for improved photovoltaic devices," *Nature Materials* Vol. 9, pp. 205-213, 2010.

[9] K. R. Catchpole and A. Polman, "Plasmonic solar cells," *Opt. Express* Vol. 16, pp. 21793-21800, 2009
[10] R. A. Pala, J. White, E. Barnard, J. Liu, and M. L. Brongersma, "Design of Plasmonic Thin-Film Solar Cells with Broadband Absorption Enhancements," *Adv. Mater*. Vol. 21, pp. 3504–3509, 2009.
[11] C. Jeong, P. Nair, M. Khan, M. Lundstrom, and M. A. Alam "Prospects for Nanowire-Doped Poly-crystalline Graphene Films for Ultratransparent, Highly Conductive Electrodes", *Nano Lett*., Vol. 11, pp. 5020–5025, 2011.
[12] D. A. G. Bruggeman, "Calculation of various physical constants of heterogeneous substances. I. dielectric constants and conductivity of mixed bodies from isotropic substances," *Ann. Phys.* Vol. 24, 636-664, 1935.
[13] P. Sheng, "Theory of the dielectric function of granular composite media," *Phys. Rev. Lett.* Vol. 45, 60-63, 1980.
[14] K. R. Catchpole, S. Mokkapati, F. Beck, E-C Wang, A. McKinley, A. Basch, and J. Lee, "Plasmonics and nanophotonics for photovoltaics", *MRS Bulletin* Vol. 36, pp 461-467, 2011
[15] P. Etchegoin, E. Le Ru, and M. Meyer, "An analytic model for the optical properties of gold," *J. Chem. Phys.*, Vol. 125, pp. 164705-3, 2006.
[16] X. Ni, Z. Liu, and A. V. Kildishev, "PhotonicsDB: Optical Constants," doi: 10254/nanohub-r3692.10, 2007.
[17] L. J. Prokopeva, J. Borneman, and A. V. Kildishev, "Optical dispersion models for time-domain modeling of metal-dielectric nanostructures," *IEEE Trans. Magn.* Vol. 47, pp 1150-1153, 2011.
[18] L. J. Prokopeva, A. V. Kildishev, J. Fang, J. Borneman, M. D. Thoreson, V. M. Shalaev, and V. P. Drachev, "Nanoplasmonics FDTD Simulations Using a Generalized Dispersive Material Model," 27th International Review of Progress in Applied Computational Electromagnetics Symposium (ACES 2011), Williamsburg VA, 2011
[19] J. W. Schuster, and R. Luebbers, "An accurate FDTD algorithm for dispersive media using a piecewise constant recursive convolution technique," *IEEE Trans. Antennas Prop.*, Vol. 4, pp. 2018-2021, 1998.
[20] A. Taflove, and S. C. Hagness, *Computational Electrodynamics: The Finite-Difference Time-Domain Method,* Artech House, 2005.
[21] A. V. Kildishev, U. Chettiar, and V. M. Shalaev, "Simulation of Optical Negative Index Materials Using Parallel FDTD Method," 22th International Review of Progress in Applied Computational Electromagnetics Symposium (ACES 2006), Miami FL, 2006
[22] M. D. Thoreson, J. Fang, A. V. Kildishev, L. J. Prokopeva, P. Nyga, U. K. Chettiar, V. M. Shalaev, and V. P. Drachev, "Fabrication and Realistic Modeling of 3D Metal-Dielectric Composites, " *J. Nanophotonics*. Vol. 5, pp. 0515131-17, 2011.
[23] A. K. Sarychev, and V. M. Shalaev *Electrodynamics of metamaterials*, World Scientific, 2007